



A Chamber for Analogues of Planetary Surfaces Laboratory: the CAPSULA project

S. De Angelis¹, E. La Francesca¹, M.C. De Sanctis¹, M. Casalini², G. De Astis³,
G. Agrosi⁴, T. Di Iorio⁵, M. Ferrari¹, M. Formisano¹, A. Frigeri¹, P. Manzari⁶, V.
Moggi Cecchi², G. Pratesi², G. Tempesta⁴, D. Biondi¹, and A. Boccaccini¹

¹ National Institute for Astrophysics – Institute for Space Astrophysics and Planetology,
INAF-IAPS, via Fosso del Cavaliere 100, Rome, 00133, Italy

² University of Florence, Dept. Earth Sciences

³ INGV - Rome

⁴ University of Bari, Dept. Earth and Geoenvironmental Sciences

⁵ ENEA - Rome e-mail: simone.deangelis@inaf.it

Received: 26 March 2024; Accepted: 15 May 2024

Abstract. The comprehension and interpretation of VIS-IR spectra from space missions to Solar System rocky bodies is generally based on the qualitative/quantitative comparison with standard laboratory datasets, i.e. spectra often acquired in laboratory at room pressure/temperature, dominated by water bands. We developed a new laboratory setup CAPSULA (Chamber for Analogues of Planetary Surfaces Laboratory), consisting of an environmental chamber equipped with a FTIR spectrometer to acquire spectra of planetary analogues in various conditions. The chamber allows to obtain (i) high vacuum ($< 10^{-6}$ mbar); (ii) high (> 800 K) and cryogenic T (< 50 K). With this setup we can study planetary analogues of terrestrial planets surfaces as well as of icy moons and meteorites in a wide spectral range and in different environmental conditions. The opportunity of acquiring spectra on analogs and meteorites in the lab in conditions similar to extra-terrestrial environments is key to improving our interpretation of spectra acquired remotely from orbital and landed missions at remote sites in our Solar System.

Key words. Laboratory VIS-IR spectroscopy – Planetary analogues – Meteorites

1. Introduction

Space missions for minor bodies exploration in the last decade have enormously enhanced our knowledge on the internal structure, composition and evolution of both asteroids and comets. In particular, asteroids of various sizes have been and are currently investigated as

targets of many space missions, both in the Main Belt and in the region of the Near Earth Asteroids. NASA/Dawn mission explored the Main Belt objects Vesta and Ceres (Russell & Raymond (2011)), while NASA/Psyche will orbit the metallic asteroid Psyche with several instruments (Elkins-Tanton et al. (2016)). JAXA/Hayabusa and Hayabusa2 (Abe et al.

(2012)) spacecrafts returned samples from Itokawa and Ryugu Near Earth asteroids (Yada et al. (2021), Dartois et al. (2023), Kimura et al. (2024), Yesiltas et al. (2024)), respectively, and in the next future the NASA/OSIRIS-Rex (Lauretta et al. (2015)) will make available returned Bennu samples.

In the last few years, cometary missions have provided extremely relevant data; in 2006, the NASA/Stardust spacecraft delivered dust ejected from the nucleus of comet 81P/Wild 2 (Brownlee (2014)), a Jupiter-Family comet that accreted in the Kuiper Belt. Laboratory analysis of collected cometary material provided important information on numerous astronomical phenomena resulting relevant also for the subsequent cometary mission ESA/Rosetta (Barucci & Fulchignoni (2017)). In the near future, ESA/JUICE (Grasset et al. (2013)) and NASA/Europa Clipper (Daubar et al. (2023)) will investigate the icy moons Ganymede and Europa. Laboratory measurements in environmental conditions similar to those of the mission targets will be fundamental for the interpretation of the spectral data that will be obtained from the icy moons. Data obtained from in-flight spectrometers, and observations from Earth-based telescopes, as well as laboratory analyses of returned particles, have revealed with detail the surface composition of many planetary bodies. Nevertheless, much laboratory work is still required in order to correctly interpret the data acquired from spectrometers in the visible, near- and mid-IR range. Observational data are routinely compared with literature spectral datasets that are often acquired at standard laboratory conditions, i.e. room pressure and temperature.

Data acquired with VIR/Dawn at Ceres in the 3- μm region for example showed that the dwarf planet is covered with hydrous and NH_4 -bearing minerals, as implied by the 2.7- μm absorption band present in spectra on its surface (de Sanctis et al. (2015), de Sanctis et al. (2016)). Recent spectral data from OVIRS onboard OSIRIS-REx at asteroid Bennu and from Hayabusa2 spacecraft at Ryugu also show the presence of hydrous phases across the surfaces of such bodies, testified by a broad absorption band at 2.7 μm (Hamilton et al. (2019),

Kitazato et al. (2019)). Laboratory reflectance spectra of phyllosilicates and meteorites in the 3- μm region are often obtained at room P-T conditions: in that case this spectral region is dominated by absorptions of ambient water adsorbed on the sample [Che et al. (2011), Takir et al. (2013), Beck et al. (2010), Beck et al. (2018)]. Considering the spectra of carbonaceous chondrites the 3- μm absorption bands are in almost all cases due to terrestrial water contamination. In such cases (i) the comparison of observational with laboratory data is often very difficult and the interpretation hard, and (ii) the important spectral information carried by the original phyllosilicate in the chondrite (identified by the narrow absorption located at $\sim 2.7\text{-}\mu\text{m}$) is hidden by the terrestrial water (responsible of a broad and intense absorption near 3- μm). New laboratory work should address several open questions, such as (i) the study of VIS-IR reflectance spectra of hydrated minerals and organics in high vacuum and at cryogenic/high temperatures; this is important to understand absorptions in spectra of NEA, Main Belt or TNO objects, as well as of the icy moons. The unambiguous identification of the hydrated phases on the surfaces of minor bodies has importance in deciphering the thermal history of such objects, in that different mineralogical associations can imply different evolutions. (ii) The investigation of thermal stability of NH_4 -phyllosilicates at high temperatures would give hints about the geological evolution of bodies like Ceres or others in the outer Solar System. The identification of the ammonium-bearing phase would provide hints about the formation of the body, the degree of thermal alteration that materials experienced. (iii) The experimental estimate of the hydration or ammonium content in such minerals, through analysis of absorption bands. (iv) The laboratory spectral analyses at variable P-T conditions on returned asteroidal samples (i.e. from OSIRIS-REx and Hayabusa2 missions (Yada et al. (2021), Dartois et al. (2023))) would provide additional precious information about their composition and history, thus for example in providing clues about the nature and abundance of volatile content. (v) The spectral analyses of carbonaceous chondrites

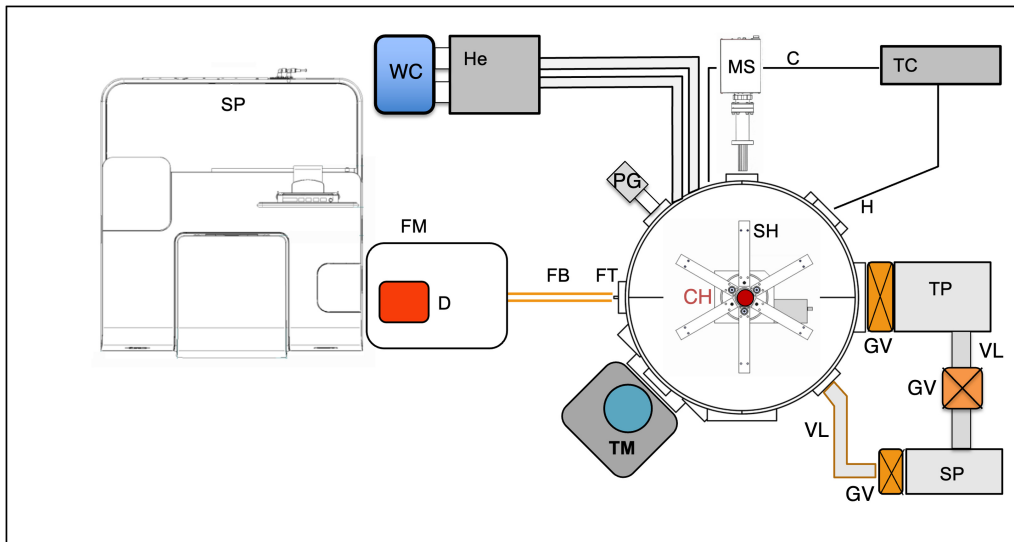


Fig. 1. Schematic view of the experimental apparatus. SP: spectrometer. FM: fiber module. D: detector. FB: fiber bundles. FT: optical feedthrough. TM: port dedicated to Transmission Module (not present). SP: scroll pump. TP: turbomolecular pump. GV: gate valves. VL: vacuum line. PG: pressure gauge. CH: Cold Head. SH: sampleholder. TC: thermal controller. C: low temperature control line. H: high temperature control line. MS: mass spectrometer. He: gas helium compressor. WC: water cooling for helium compressor.

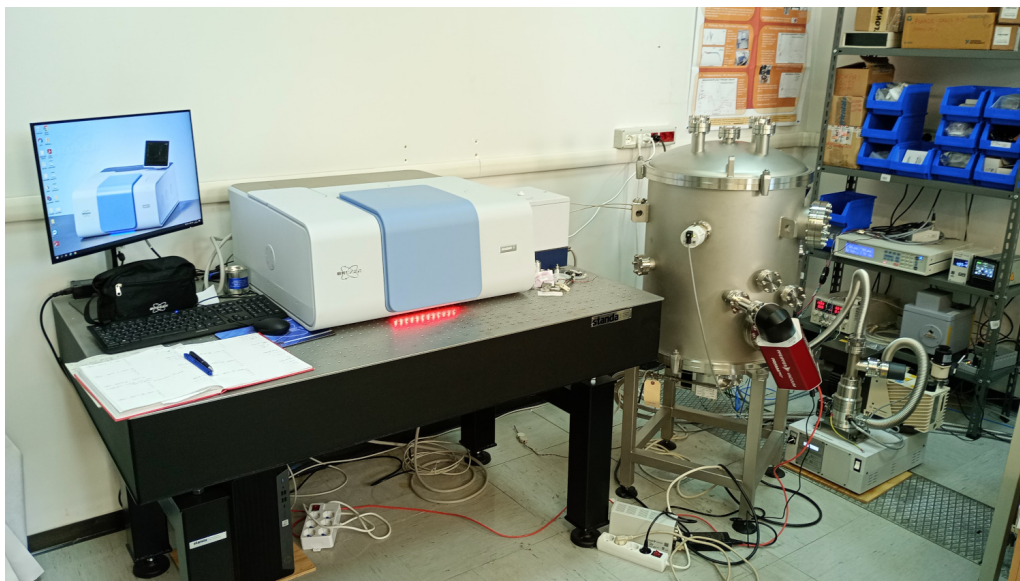


Fig. 2. CAPSULA experimental apparatus, with the FTIR spectrometer linked to the vacuum chamber through optical fibers.

and other types of meteorites in the infrared range carried out at high temperatures would

provide constraints for the determination of the content of hydrous phases; this will help in the



Fig. 3. CAPSULA Thermal Vacuum Chamber. The Mass Spectrometer (red block containing the electronics) is visible.

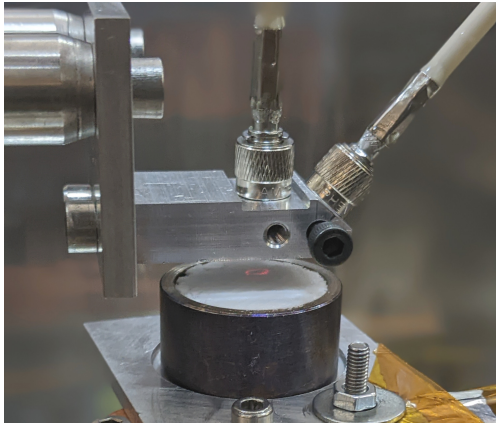


Fig. 4. Geometry of fiber bundles used for sample illumination and light recollection inside the TVC.

comparative study of observational data from asteroids and laboratory data on meteorites, giving a potential contribution to the question of asteroid-meteorite link (Greenwood et al. (2020)).

In this paper we first describe the experimental apparatus that has been developed at IAPS-INAF laboratory; then the main commissioning tests that have been performed in order to check the performances of all the principal subsystems; finally a few preliminary measurements on some mineral samples are presented. The novelty of such a laboratory setup with respect to existing others is (i) the possibility to simultaneously process and analyse multiple samples, (ii) the wide temperature range that can be reached in the chamber, from cryogenic up to high temperatures, (iii) the possibility to combine simultaneously spectral and mass spectrometry measurements, (iv) the capability to measure the reference target directly in vacuum, thus minimizing environmental artifacts (i.e. water vapour and CO₂ residual absorptions) on samples spectra.

2. The Experimental Setup: CAPSULA

The CAPSULA setup is hosted at INAF-IAPS C-Lab laboratory (Figure 1). It is constituted by a Fourier Transform Infrared (FTIR) spectrometer, equipped with a large Thermal Vacuum Chamber (TVC), in which the samples to be processed and analyzed are placed (Figure 1 and Figure 2). In the following sections the apparatus subsystems are described.

2.1. Spectrometer

The core instrument of the experimental apparatus is a Bruker Invenio R Fourier Transform InfraRed (FTIR) interferometer. It is a modular instrument with two different internal light sources, a Near InfraRed (NIR) for illumination up to $\sim 5 \mu\text{m}$ and a Mid-InfraRed (MIR) Globar source for illumination beyond $\sim 5 \mu\text{m}$. A room temperature detector (DLATGS, 10 kHz) can be used in the range $<1\text{--}20 \mu\text{m}$, while a liquid nitrogen (LN₂) Mercury Cadmium Telluride (MCT) detector is used in the $<1\text{--}14 \mu\text{m}$ spectral range, characterized by higher velocity (20 kHz) and Signal to Noise Ratio. An external fibers module allows to interface the spectrometer with optical fibers in order to per-

Table 1. Parameters of experimental setup.

Parameter	Description	Range	Configuration
Detector	LN ₂ cooled MCT	1 – 6 μ m	MCT + fibers
//	//	1 – 14 μ m	MCT + mirrors
//	room-T DLaTGS	1 – 6 μ m	DLaTGS + fibers
//	//	1 – 20 μ m	DLaTGS + mirrors
Fiber Core	InF ₃	200 μ m	single fiber
Bundle	Peek	0.3 – 6 μ m	19 fibers
Low Temperatures	Gas ⁴ He	9-300K	Compressor+Cryocooler
High Temperatures	heaters	300-1073K	Si ₃ N ₄
Pressure	-	10 ³ – 10 ⁻⁷ mbar	at room T
//	-	10 ³ – 10 ⁻⁸ mbar	at cryogenic T
Mass Spectrometer	Prisma Pro	1 – 200 amu	QMG 250 M 90°
NIR source	QTH	0.3 – 4.8 μ m	-
MIR source	Globar	1.2 – 20 μ m	-
Illumination geometry	-	-	$i = 40^\circ, e = 0^\circ$
Spatial Resolution	-	-	$i, e \approx 3mm$
Spectral Resolution	-	0.16 – 4cm ⁻¹	

form measurements on samples placed outside the instrument sample compartment.

2.2. Vacuum Chamber

The Vacuum Chamber is a vertical cylinder with dimensions 50 cm in diameter and 60 cm high (Figure 3). The TVC is mounted on a 40 cm high mechanical support placed in front of the optical bench that hosts the spectrometer. A number of entry ports (several DN40CF, one 63CF and four 100CF) are placed around the TVC on all sides in order to allow the mounting of viewports, connect the pumping line, light transmission, electrical connections, cooling system and other functionalities. The top cover is removable in order to put the samples inside the chamber. A calcium fluoride (CaF₂) window mounted on a DN100CF port is used to visually control the inside of the TVC during operations.

2.3. Illumination and Geometry

The setup is designed to acquire reflectance spectra. The chamber and the spectrometer are coupled by means of two optical fiber bundles, both composed by 19 fibers, each with 200/260- μ m core/cladding respectively. Both fiber bundles are covered with a peek jacket, with length ~ 47 cm in the air side and >50 cm in the vacuum side. The fibers, in Indium Fluoride Glass (InF₃), allow the signal to be transmitted in the 0.35-6 μ m range. A future instrumental upgrade foresees the spectral range extension towards the mid-IR by means of use of mirrors instead of fibers. One fiber bundle (illumination) is connected through the exit port of the FTIR to its internal light sources (NIR or MIR source). The other fiber bundle (collection) recollects the light from the sample and is connected to the entry port of the FTIR. In order to transmit the light in/from the interior of the TVC, the fiber bundles pass through a Conflat CF40 optical feedthrough; the couple of bundles with the optical feedthrough have been designed and realized custom, and the bundles pass through the

feedthrough without any interruption in order to minimize the signal losses. The illumination spot on the sample (at angle of 40°) and the collection spot (at 0°) are about 2 mm (Figure 4). A custom mechanical support has been realized at IAPS workshop for the fibers. This particular geometric configuration has been chosen with the aim of having the illumination and collection fibers as close as possible to each other, in order to maximize the signal.

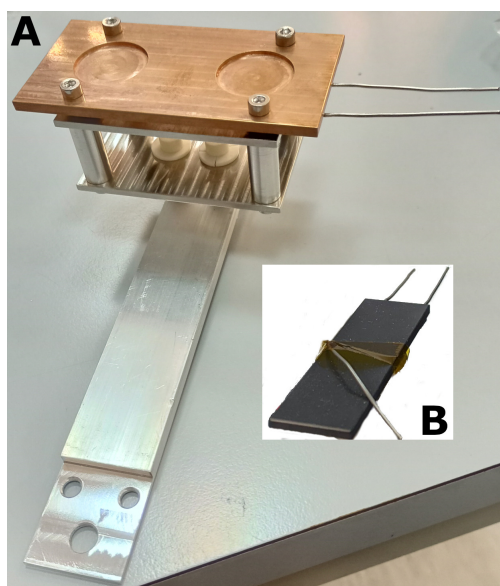


Fig. 5. A: heating system with thermal decoupling supports and copper sample cups plate; the heater is compressed below the top copper plate. B: Si_3N_4 heater.

2.4. Pumping System

The pumping system consists of a primary scroll pump for the initial rough vacuum down to $\sim 10^{-3}$ mbar, coupled with a turbomolecular pump (1100 Hz) for high vacuum down to $\sim 10^{-7}$ mbar (at room temperature). Two electro-pneumatic gate valves with DN40CF (rough pump) and DN100CF (turbo pump) dimensions commanded via LabVIEW software permit to obtain the final pressure along the vacuum line. The turbomolecular pump is con-

nected through the back side to the scroll pump with an intermediate manual gate valve. A Pirani-Cold Cathode gauge connected to the TVC is used as pressure sensor and interfaced via LabVIEW for pressure data visualization and saving. Finally a further manual gate valve is used to allow air inlet in the chamber (venting) if necessary.

2.5. Heating System and High Temperature Control

A heating system consisting of five rectangular Si_3N_4 heaters, placed just below copper sample-holders cups, allows to heat samples up to 1073K in high vacuum. Each heater is 20x70 mm in size and allows heating two samples cups. Custom sampleholder have been designed and realized in order to accommodate the heaters in the internal chamber sampleholder. The heaters are pressed between a stainless steel plate (below) and a copper plate (above) in a system designed (Figure 5) such that heat dissipation is maximized towards the top direction: the samples to be heated and analyzed are placed in copper cups hosted on the copper plate (Figure 5). The heater and copper plate are thermally decoupled by means of ceramic cylinders from the supporting aluminum bars. The high temperature control system is based on a PID (Proportional-Integral-Derivative) controller, one for each heater element. In order to enable/disable the current passage and then the heating, the PID is connected to a Solid State Relay and a 48V AC transformer. Type K thermocouples (Nickel-Chromium / Nickel-Alumel) are used as temperature sensors for the high temperature range (above 300K) monitoring and control.

2.6. Cooling System and Cryogenic Temperature Control

The samples are cooled down at cryogenic temperatures by means of a gas line ^4He compressor (closed cycle) with a two-stage Sumitomo Gifford-McMahon Cold Head (Figure 7), that enters in the TVC through a 100 CF flange. The cryocooler must be in

turn cooled down with liquid water, and this is done by means of a chiller by Applied Thermal Control ltd (ATC), which supplies water in a closed cycle at a temperature of 14° C. The samples are placed into copper cups with 20 mm diameter, and mounted on copper horizontal bars that build the sampleholder. A factory calibrated Si-Diode cryogenic sensor is used for monitoring the cold head temperature in the low-T range, while a Cernox (negative sensor, calibrated in the laboratory) is used to control the temperature of the cooled sample. A 25 Ω 100W heater resistance mounted on the cold head (Figure 6) is used to perform stepped temperature ramps from cryogenic up to room value. Both the cryogenic sensors and the resistance heater are handled by means of a Lakeshore controller and managed via LabVIEW from a dedicated pc.

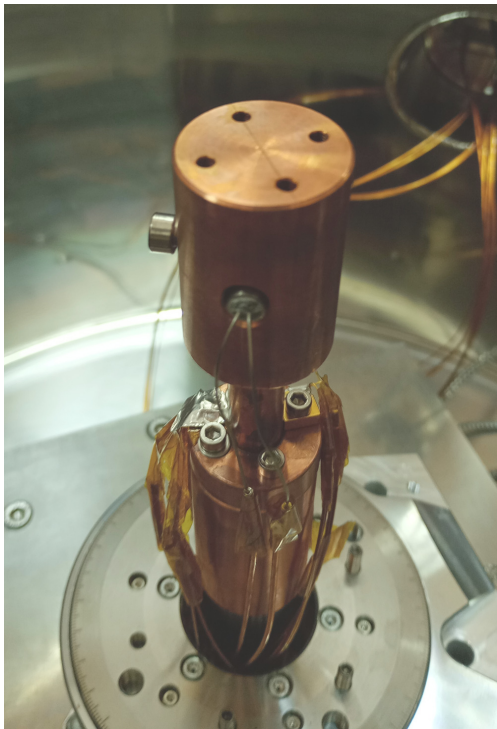


Fig. 6. Two-stage Cold Head inside the TVC.

2.7. Reference Targets

The reference targets should be measured in laboratory conditions that are the more similar possible to the conditions in which the samples are analyzed. In the case of samples that are analyzed in vacuum, it is important that also reference targets are measured in the same vacuum conditions (and also illumination, etc...). In this way the telluric bands due to H₂O vapour and CO₂ absorptions are well compensated in the reference signal. In order to accomplish this task, custom reference targets suitable for use in UHV conditions have been realized by Labsphere, in particular a UHV Spectralon 99% and an Infragold. Both targets have been realized custom in order to fulfil the size and height available in the sampleholder cups and to meet the requirements of having the top surface at focus.



Fig. 7. UHV Infragold realized for IR reference measurement in vacuum.

2.8. The Sampleholder

A custom sampleholder has been designed and realized at the premises of IAPS mechanical

workshop. The sampleholder has the following requirements: (i) it must hold the samples to be heated; heat flow from heaters must be maximized towards hot samples (up); (ii) the heating system must be thermally insulated from the rest of the supports; (iii) it also must hold the samples to be cooled down; the supporting plates of cold samples are thermally connected to the cryocooler Cold Head. The whole sampleholder is mounted upon a UHV rotation stage placed on the bottom of the chamber, and can rotate along its central vertical axis in order to put the sample to analyze in the correct illumination configuration. The thermal contact between the cold samples and the Cold Head is assured by means of flexible OFHC (oxygen-free high thermal conductivity) copper thermal straps.

2.9. Mass Spectrometer

A mass spectrometer (Prisma Pro from Pfeiffer Vacuum, QMG 250 M 90° model) is installed on a port of the vacuum chamber. The detector used is a C-SEM/Faraday, with mass range 1-200 amu and resolution 0.5-2.5 amu. The mass spectrometer is only switched on and used in high vacuum at pressures lower than 5×10^{-5} mbar. The detection limit (lowest detectable partial pressure) is 3×10^{-15} mbar. It is used with the aim of monitoring and measuring the volatile species that are emitted during the processing of materials. The evaluation and measuring of the outgassed chemical species, and their decomposition products, is performed during the thermal processing of materials, both at high and low temperatures, also with the aim of quantifying the influence of temperature of such processes. The instrument can be used mainly in two modalities: (i) by acquiring continuously mass spectra and following the changing of a spectrum vs. time (i.e. mass (amu) along X-axis and Partial Pressure along Y-axis); (ii) by selecting multiple chemical species of interest (both atoms and molecules) and by following the change in time of their peak Partial Pressure (Y-axis) vs. time (X-axis).

3. Preliminary Tests and Measurements

3.1. Functionality Tests

3.1.1. Illumination tests

The transmittance of the fiber bundles has been extensively measured in the laboratory in the whole nominal spectral range of effective transmission of the fibers, that is $0.3 - 5.5 \mu\text{m}$. The transmittance in the $0.3 - 1 \mu\text{m}$ has been measured by means of ASD FieldSpec4 spectrometer, by connecting the fibers to the exit port of a QTH (Quartz Tungsten Halogen) light source, with a Thorlabs collimator with SMA connection on the other side, and illuminating a Labsphere Spectralon99 white panel; the reflected signal was then collected with the FieldSpec input fiber bundle; this measure was first performed with a single illumination fiber (used as reference measure) connected to the light source, and then it was repeated by connecting the first fiber with a second (test) fiber. The ratio of the two measurements allows to obtain the test fiber optical transmittance. The IR transmittance in the $1 - 5.5 \mu\text{m}$ has been estimated by using the fiber optics module coupled with the FTIR setup. The overall transmittance is of the order of 80% La Francesca et al. (2023b).

3.1.2. Vacuum tests

The first functionality tests have been performed in order to check the correct working of the pumping system and the overall vacuum line and chamber. The vacuum measurement has been performed during the cryogenic temperature sensors calibration (see next session). The procedure used for producing high vacuum in the chamber consisted in the following steps: (i) start the scroll pump for rough vacuum; (ii) in this phase only the electropneumatic 40 CF gate valve connecting the scroll pump to the chamber is open, while all the other valves are kept closed; (iii) when the rough vacuum in the TVC reaches approximately 10^{-3} mbar both the 100 CF e.p. gate valve and the turbo pump back valve are opened, in order to start to pump also

through the line across the turbo pump; this can cause a slight temporary increase of pressure in the chamber, followed by a rapid decrease; (iv) when the limit pressure with the scroll is reached ($\sim 10^{-3}$ mbar) the turbomolecular pump is also switched on; (v) once the turbo pump is starting, the e.p. 40 CF gate valve is closed, and only the 100 CF valve is kept open on the chamber (together with the turbo pump rear valve); (vi) finally high vacuum is reached with a ultimate pressure of about $\sim 10^{-7}$ mbar, at cold temperature (Figure 8).

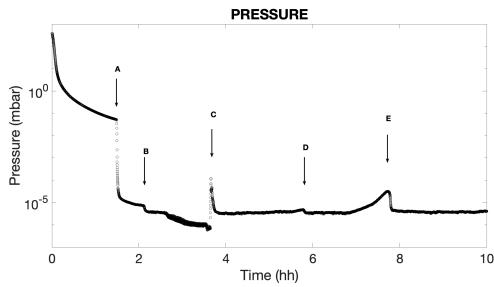


Fig. 8. Vacuum performances test. A: start of turbomolecular pump. B: start of cooling. C: stop cooling. D and E: outgassing in TVC due to temperature rising.

3.1.3. Cryogenic sensor calibration and Low Temperature tests

In order to calibrate the Cernox temperature sensor (range down to 20K), this has been mounted on the top of the Cold Head in a position as close as possible to the factory calibrated Diode sensor (range 1.4 - 325K). Both sensors have been fixed with screws, in order to assure the thermal contact with the Cold Head, and covered with kapton and aluminum ribbon in order to reduce the thermal load from outside. Both sensors were connected to the Lakeshore temperature controller and monitored via LabVIEW. While the calibrated diode sensor produce data that are already in correct kelvin units, the uncalibrated Cernox sensor initially produces raw data in resistance (Ω) units; moreover being a negative sensor, the measured resistance increases with

decreasing temperature. In order to perform a temperature test ramp at cryogenic temperatures, the procedure consisted of the following steps: (i) vacuum was initially performed according to the procedure described in 3.1.2; (ii) to start the cooling cycle, first the chiller is switched on, in order to start cooling down the Sumitomo cryocooler; (iii) then the compressor is switched on, and it starts to pump helium gas in the closed loop to the Cold Head. (iv) The test was done by cooling down the system down to 25K, in order to keep the Cernox sensor within its safe temperature range. Both calibrated (K) and corresponding uncalibrated (Ω) values were saved and then inserted into the Lakeshore controller, as $K - \log(\Omega)$ curve, and thus finally the Cernox calibration was performed (Figure 9). After sensor calibration, a new test was performed at low temperatures: the Cernox was mounted near the position of the sample cup (a few cm above the Cold Head), while the Diode sensor was fixed directly on the Cold Head. Then the procedure was as follows: (i) production of high vacuum, (ii) starting of the cooling process down to the minimum achievable temperature; in this case the temperature of ~ 9 K was reached on the Cold Head in a few hours, and ~ 22 K was the temperature reached on the sample cup. (iii) starting from the minimum temperature, a rising temperature ramp was performed by keeping the cryocooler switched on and using the 100W heater mounted on the Cold Head to heat progressively to bring the system at the desired higher temperatures. Several steps at $\Delta T = 20 - 30$ K have been performed from the lowest up to room temperature (Figure 10).

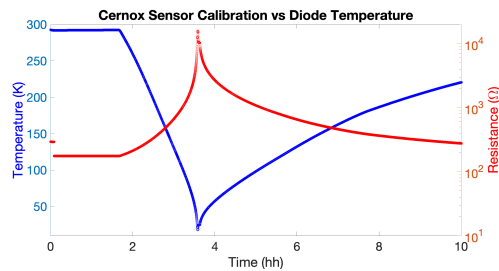


Fig. 9. Cryogenic Cernox Negative Sensor Calibration with Diode.

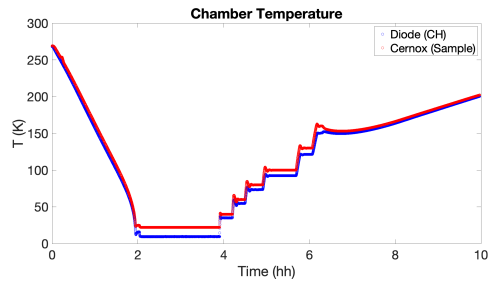


Fig. 10. Cryogenic temperatures test ramp. CH = Cold Head.

3.1.4. Mass Spectrometer Test

The mass spectrometer has been initially tested by acquiring spectra of air within the chamber, when this was maintained in high vacuum ($< 10^{-5}$ mbar) and at room temperature, without any sample placed inside (Figure 11). This acquisition must be taken into account as a *blank* measurement, consisting in the typical *background* signal due to the air within the TVC.

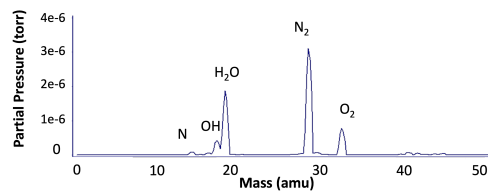


Fig. 11. Mass spectrometer acquisition test.

3.2. Preliminary Measurements

Preliminary measurements were performed with various types of natural samples, with the aim of checking the overall instrument capabilities with rocky materials in different ambient conditions, both terrestrial minerals and meteorites. Here we show as an example of first scientific data, measurements performed on three different minerals, namely three ammonium bearing compounds: (i) NH_4 -Montmorillonite (SCa3) (Ferrari et al. (2019), De Angelis et al.

(2021)), (ii) $(\text{NH}_4)_2\text{CO}_3$ (ammonium carbonate, La Francesca et al. (2023a)) and (iii) NH_4Cl (ammonium chloride, La Francesca et al. (2023a)). Spectral measurements have been carried on with the samples initially at ambient temperature and pressure, and successively changing the pressure (in vacuum); concerning the ammonium chloride, it also has been cooled down at 50K with a temperature ramp (Figure 12). The plots show how the spectra in vacuum notably change their shape, in particular for the NH_4 -SCa3 sample thanks to high vacuum much of water is removed from the sample, and the NH_4^+ absorption band near $\sim 3.1\mu\text{m}$ becomes visible (Figure 12, panel A). The ammonium carbonate (panel B) has been measured at ambient pressure and very low vacuum (a few mbar), because of its high instability in vacuum. A few millibars of vacuum is however enough to remove some of the adsorbed water and to let the NH_4^+ and CO_3^{2-} absorption features to become visible in the $3 - 5\mu\text{m}$ range. Finally the spectra of ammonium chloride (panel C) acquired in the $1 - 6\mu\text{m}$ range show the appearing of visible absorption features (at $\sim 4.1\mu\text{m}$) and the development of a band fine structure as the temperature is lowered to cryogenic values.

4. Conclusions

DESIGN AND DEVELOPMENT - All main setup subsystems have been designed and developed, namely the vacuum chamber to be coupled with the FTIR spectrometer, the light transmission system in/out the chamber (optical fiber bundles and relative feedthrough), the vacuum line, the sampleholder, the thermal control.

FUNCTIONAL TESTS - The principal subsystems have been fully tested both separately and in synergic ways. Tests have been successfully performed on the pumping system and vacuum line, illumination and spectral acquisition system, mass spectrometry and on the low/high temperature control system.

IR REFLECTANCE SPECTROSCOPY AT VARIOUS P-T CONDITIONS - Preliminary spectral measurements have been performed in the $1 - 6\mu\text{m}$ range, in vacuum and at low temperatures, on several types of samples, both terrestrial

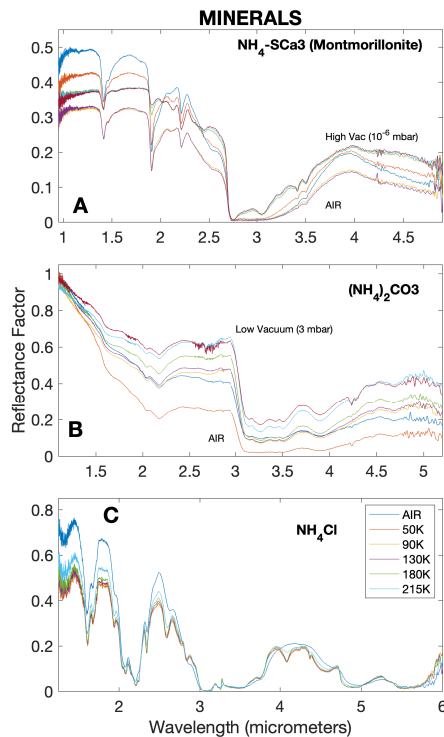


Fig. 12. Preliminary measurements on three different ammonium compounds. A: NH_4 -montmorillonite at ambient pressure and in high vacuum. B: ammonium carbonate at ambient pressure and at rough vacuum (few mbar). C: ammonium chloride in high vacuum and at various cryogenic temperatures down to 50K.

(namely a variety of NH_4 -compounds) and extraterrestrial (Martian and chondritic meteorites).

The CAPSULA setup has been designed and developed with the aim of allowing laboratory spectral studies of planetary analogues, meteorites and returned samples in environmental conditions as close as possible to planetary conditions. The described apparatus proves to be a valuable laboratory tool to be used for spectral measurements and experiments in a wide spectral range and pressure/temperature range on a large ensemble of samples of both terrestrial and extraterrestrial origin. Data acquired will be useful for both the

comprehension of physical/chemical processes on samples in the laboratory and for comparison with remote-sensing data from planetary missions.

Authors

A. Morbidini¹

Affiliations

⁶ ASI - Italian Space Agency

Acknowledgements. We acknowledge financial contribution from the Agreement ASI-INAF n.2018-16-HH.0.

References

- Abe, M., Yoshikawa, M., Sugita, S., et al. 2012, in LPI Contributions, Vol. 1667, Asteroids, Comets, Meteors 2012, ed. LPI Editorial Board, 6137
- Barucci, M. A. & Fulchignoni, M. 2017, A&A Rev., 25, 3
- Beck, P., Maturilli, A., Garenne, A., et al. 2018, Icarus, 313, 124
- Beck, P., Quirico, E., Montes-Hernandez, G., et al. 2010, Geochim. Cosmochim. Acta, 74, 4881
- Brownlee, D. 2014, Annual Review of Earth and Planetary Sciences, 42, 179
- Che, C., Glotch, T. D., Bish, D. L., Michalski, J. R., & Xu, W. 2011, Journal of Geophysical Research (Planets), 116, E05007
- Dartois, E., Kebukawa, Y., Yabuta, H., et al. 2023, A&A, 671, A2
- Daubar, I., Pappalardo, R., Buratti, B., et al. 2023, in AAS/Division for Planetary Sciences Meeting Abstracts, Vol. 55, AAS/Division for Planetary Sciences Meeting Abstracts, 311.03
- De Angelis, S., Ferrari, M., De Sanctis, M. C., et al. 2021, Journal of Geophysical Research (Planets), 126, e06696
- de Sanctis, M. C., Ammannito, E., Raponi, A., et al. 2015, Nature, 528, 241
- de Sanctis, M. C., Raponi, A., Ammannito, E., et al. 2016, Nature, 536, 54

- Elkins-Tanton, L. T., Asphaug, E., Bell, J., et al. 2016, in 47th Annual Lunar and Planetary Science Conference, Lunar and Planetary Science Conference, 1631
- Ferrari, M., De Angelis, S., De Sanctis, M. C., et al. 2019, in EPSC-DPS Joint Meeting 2019, Vol. 2019, EPSC-DPS2019-1864
- Grasset, O., Dougherty, M. K., Coustenis, A., et al. 2013, *Planet. Space Sci.*, 78, 1
- Greenwood, R. C., Burbine, T. H., & Franchi, I. A. 2020, *Geochim. Cosmochim. Acta*, 277, 377
- Hamilton, V. E., Simon, A. A., Christensen, P. R., et al. 2019, *Nature Astronomy*, 3, 332
- Kimura, Y., Kato, T., Anada, S., et al. 2024, *Nature Communications*, 15, 3493
- Kitazato, K., Milliken, R. E., Iwata, T., et al. 2019, *Science*, 364, 272
- La Francesca, E., De Angelis, S., De Sanctis, M. C., et al. 2023a, in *Asteroids, Comets, Meteors Conference 2023* (LPI Contrib. No. 2851), ACM, 2545
- La Francesca, E., De Sanctis, M. C., De Angelis, S., et al. 2023b, in XVIII Congresso Nazionale Scienze Planetarie, CNSP23, 1105
- Lauretta, D. S., Bartels, A. E., Barucci, M. A., et al. 2015, *Meteoritics & Planetary Science*, 50, 834
- Russell, C. T. & Raymond, C. A. 2011, *Space Science Reviews*, 163, 3
- Takir, D., Emery, J. P., McSween, H. Y., et al. 2013, *Meteoritics & Planetary Science*, 48, 1618
- Yada, T., Abe, M., Okada, T., et al. 2021, *Nature Astronomy*, 6, 214
- Yesiltas, M., Glotch, T. D., Kebukawa, Y., et al. 2024, *Journal of Geophysical Research (Planets)*, 129, e2023JE008090